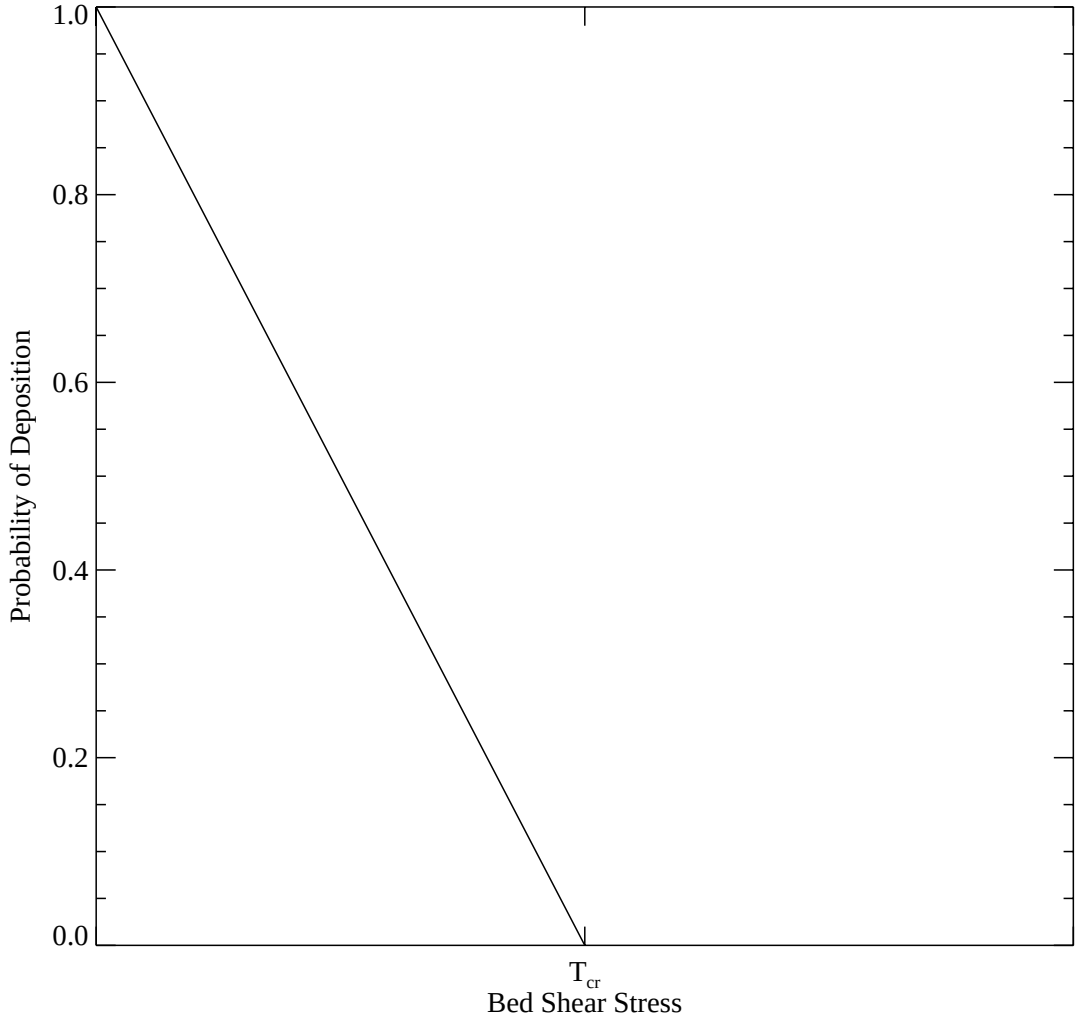

Figure A-1. Probability of deposition for cohesive sediment using the Krone formulation.

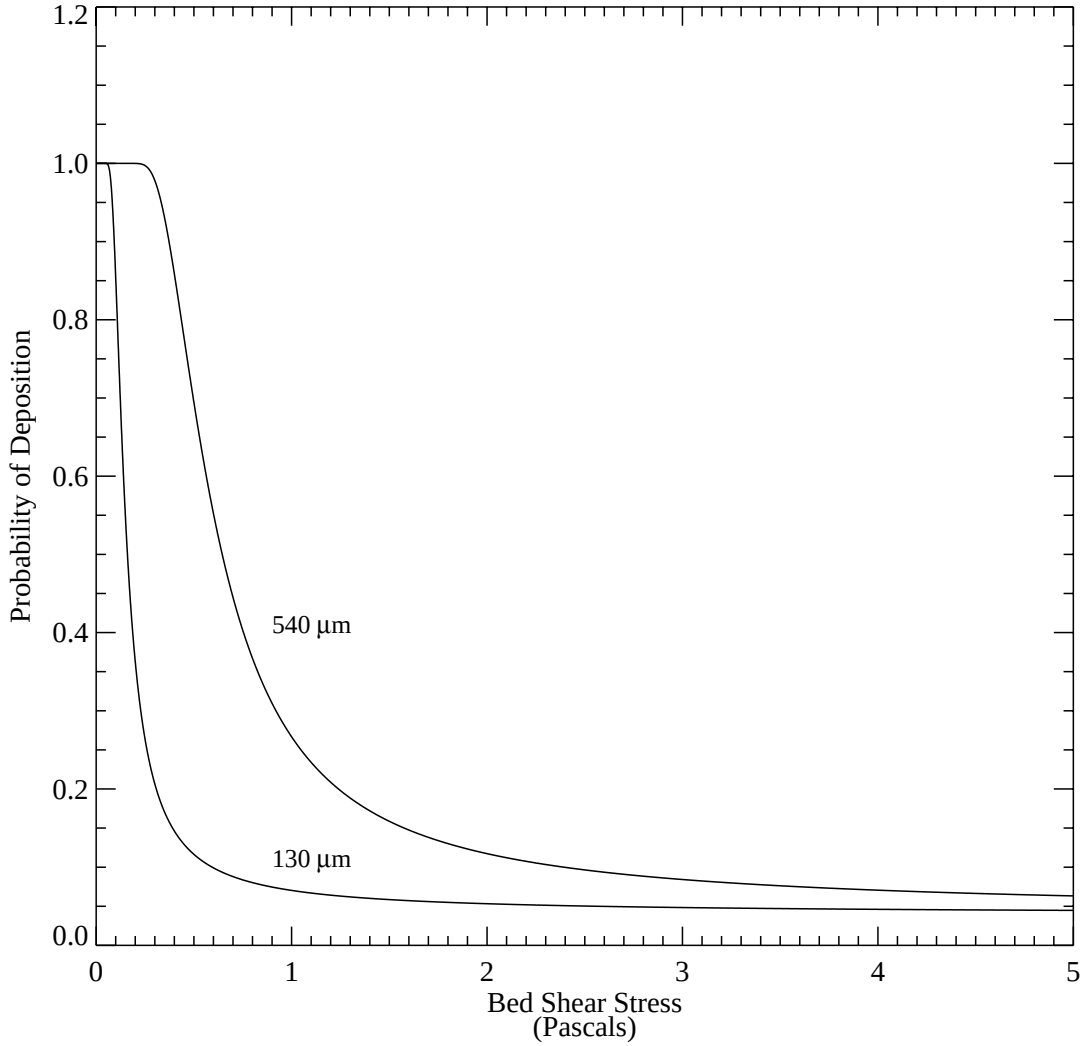

Figure A-2. Probability of deposition for non-cohesive sediment as a function of bed shear stress and particle diameter.

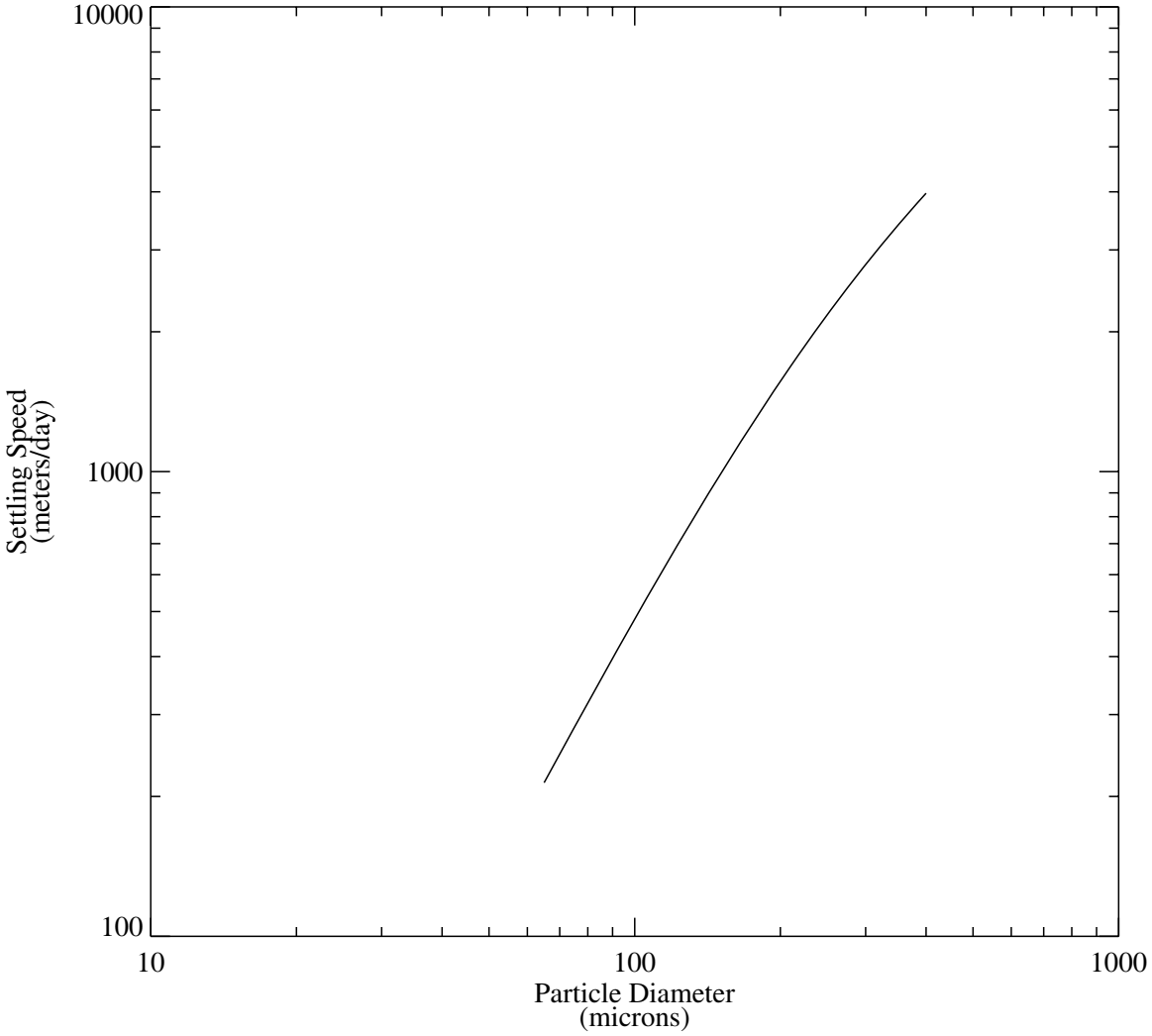

Figure A-3. Settling speed of discrete sediment particles as a function of particle diameter.

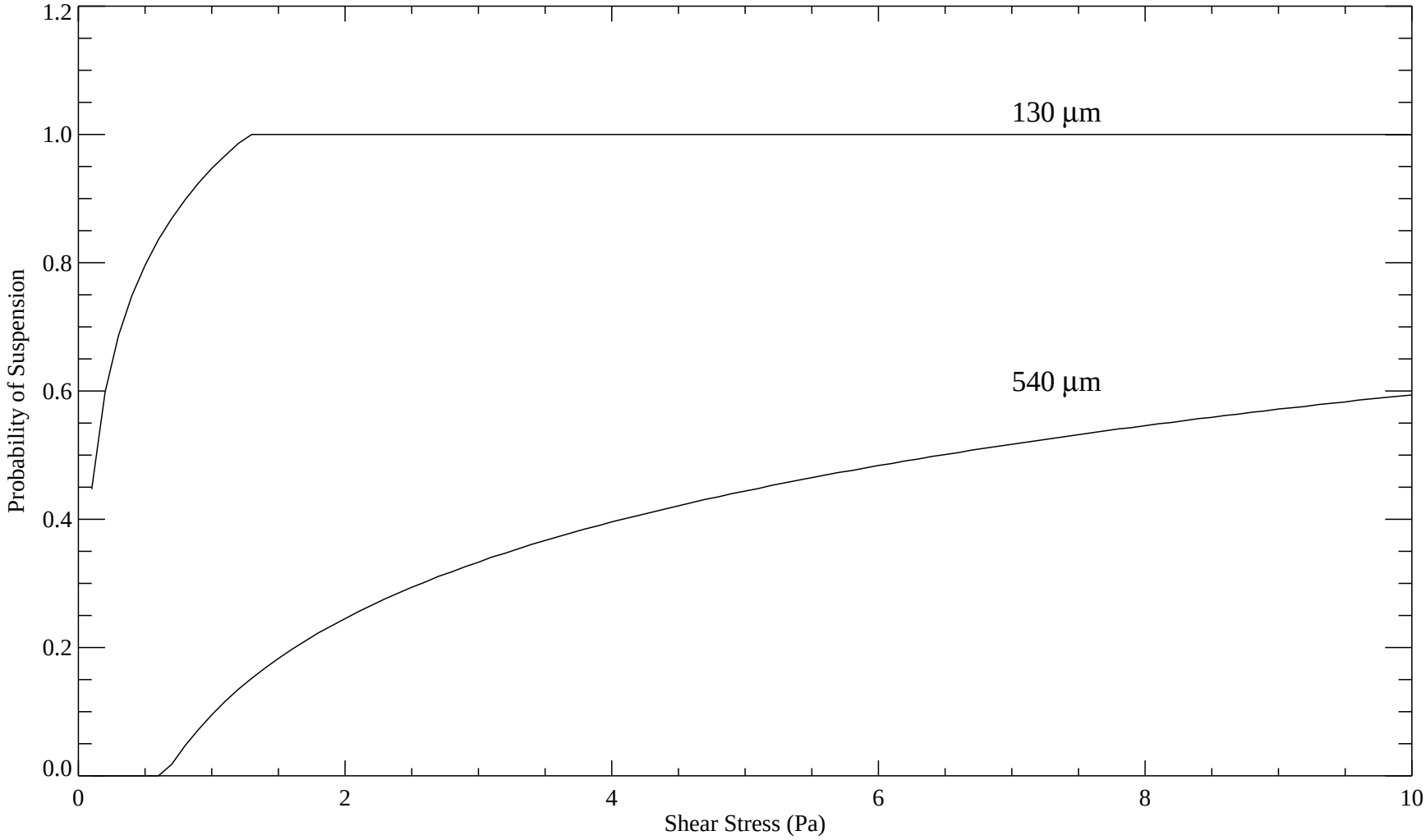

Figure A-4. Probability of suspension as a function of bed shear stress for particle diameters of 130 and 540 μm.

CO/LZ - D:\DEMpat\Analysis\Data_Analysis\Probability_resuspension\prob_suspension.pro
Thu Jun 12 16:13:34 2008

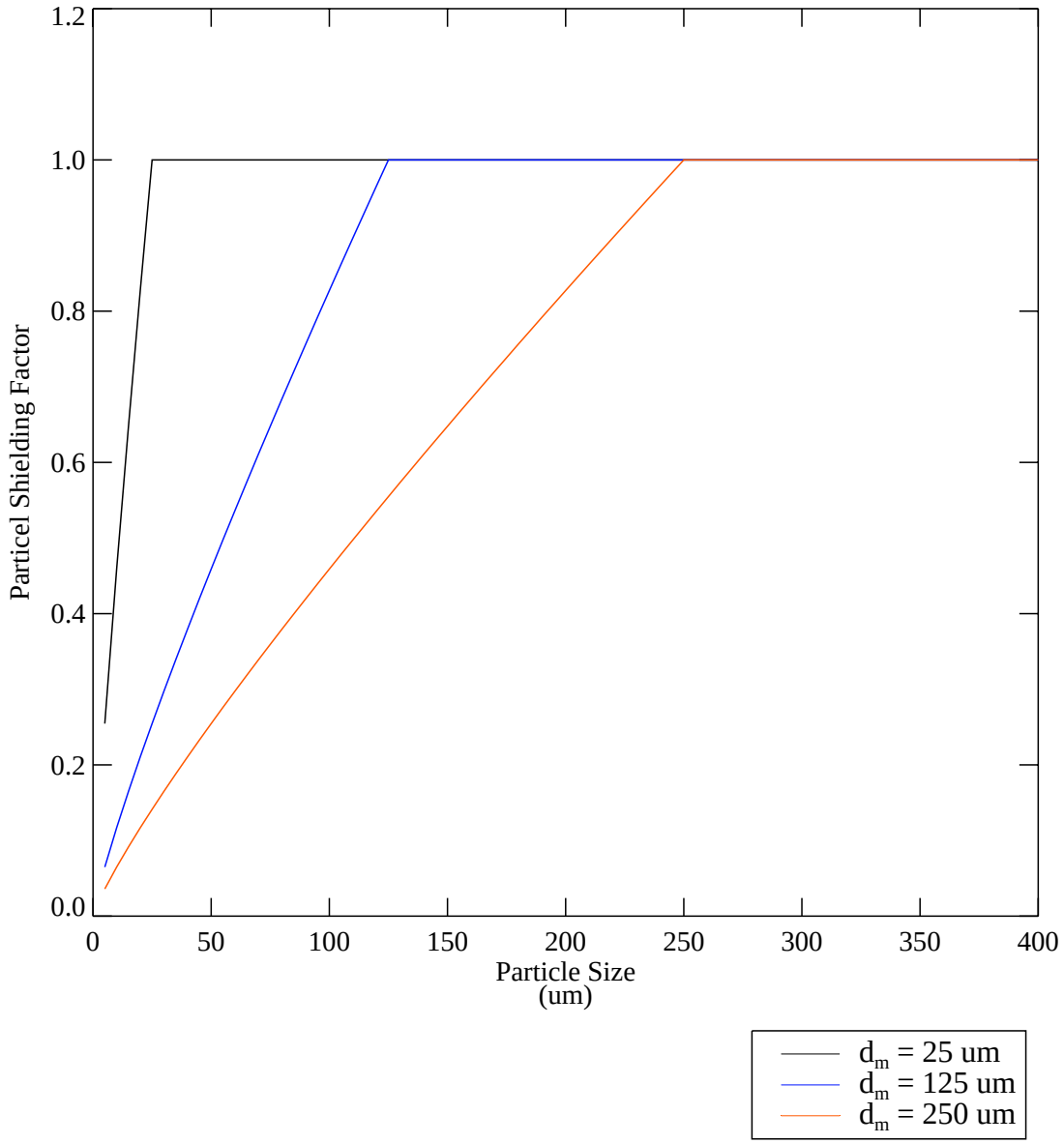

Figure A-5. Particle shielding factor as a function of particle size

Particle shielding factor is calculated as: $S_k = (d_k/d_m)^{0.85}$, *when* $d_k < d_m$, *otherwise set* $S_k = 1$.

where d_k = *particle size,* d_m = *mean particle diameter.*

FC - D:\RETldw\Analysis\hiding_factor_plot\plot_hiding_factor.pro
Thu May 01 14:52:07 2008

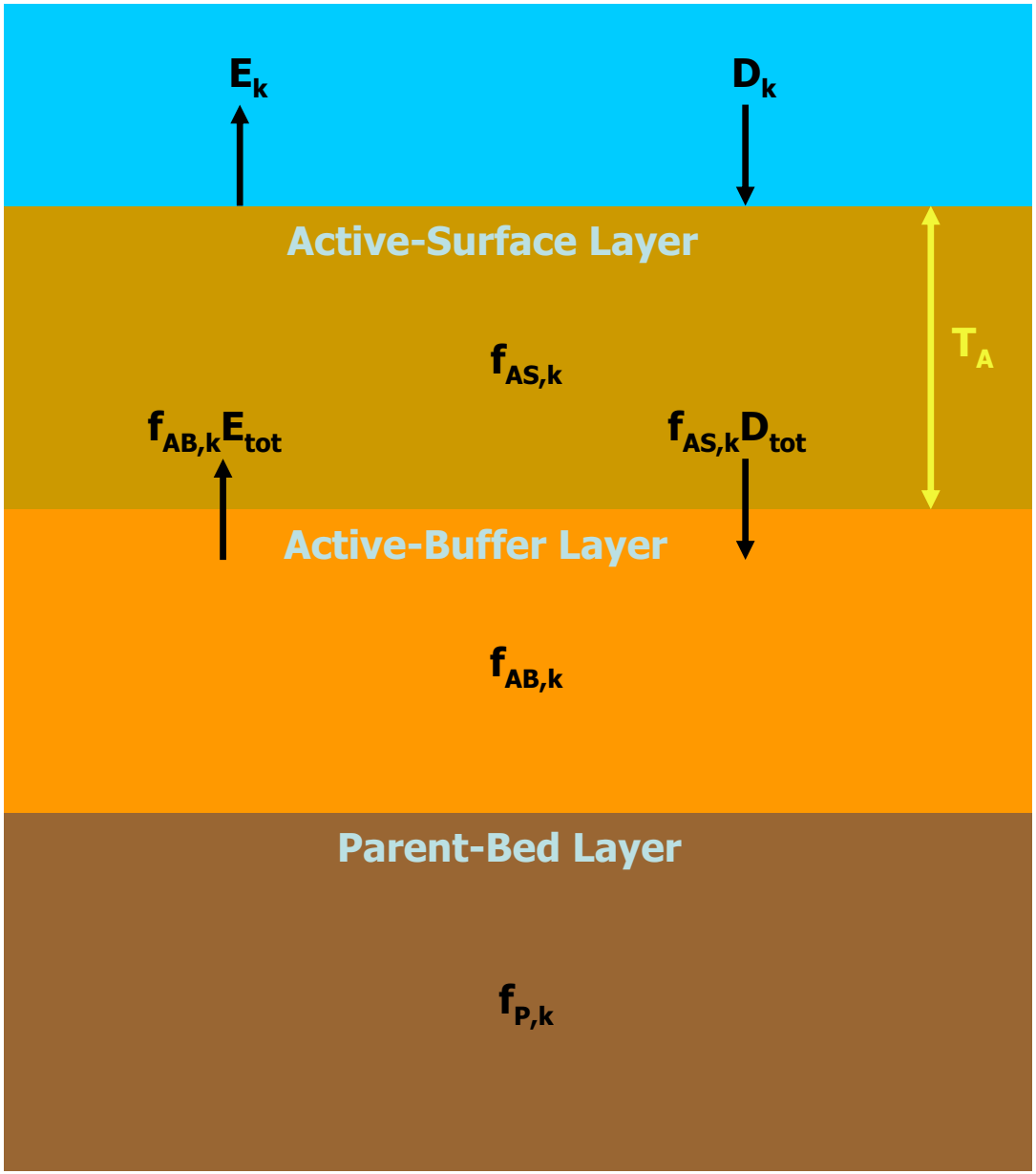

Figure A-6. Schematic of interactions between the water column, active layer, and parent-bed layer when the active-buffer layer is present.

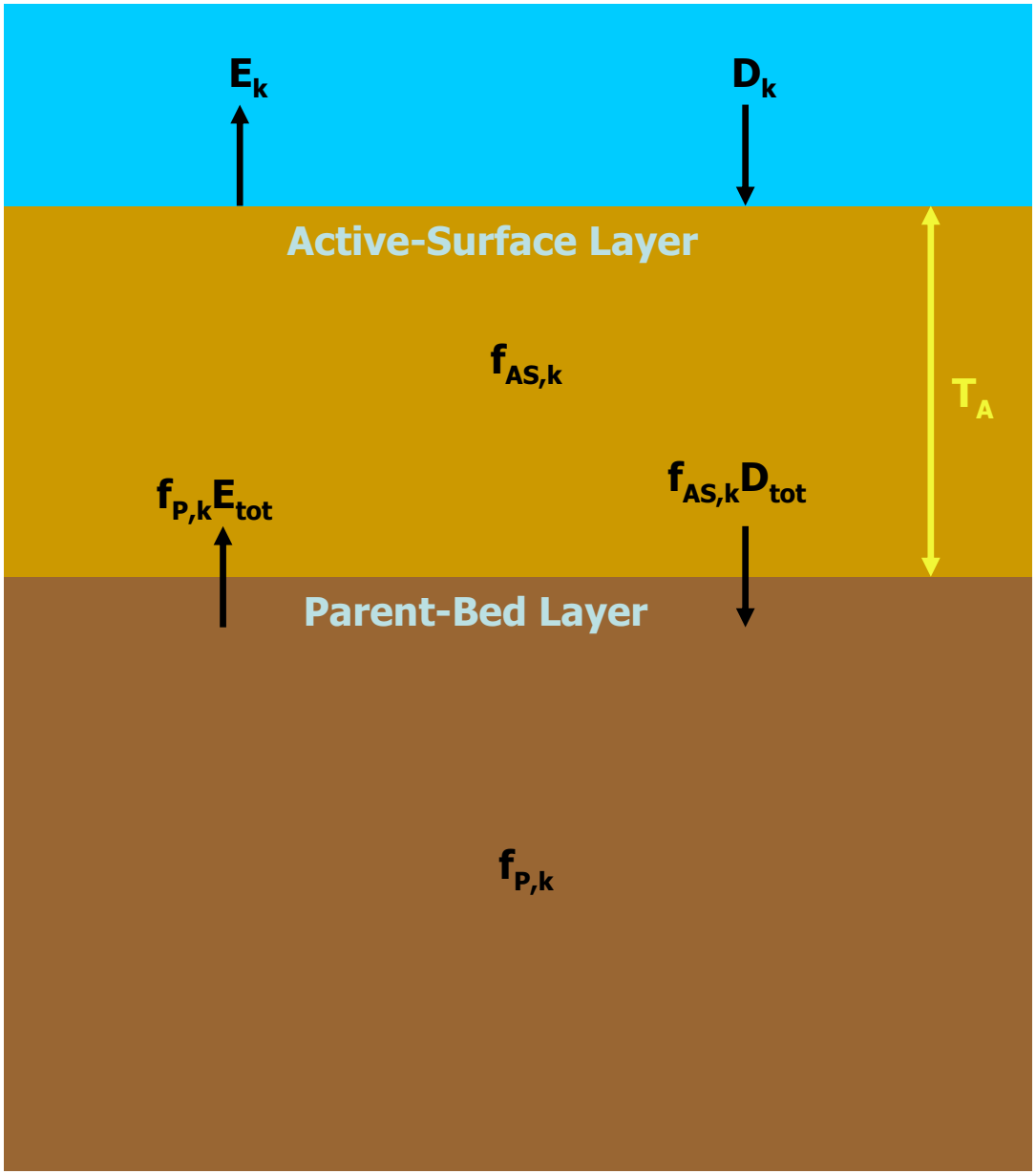

Figure A-7. Schematic of interactions between the water column, active layer, and parent-bed layer when the active-buffer layer is not present.

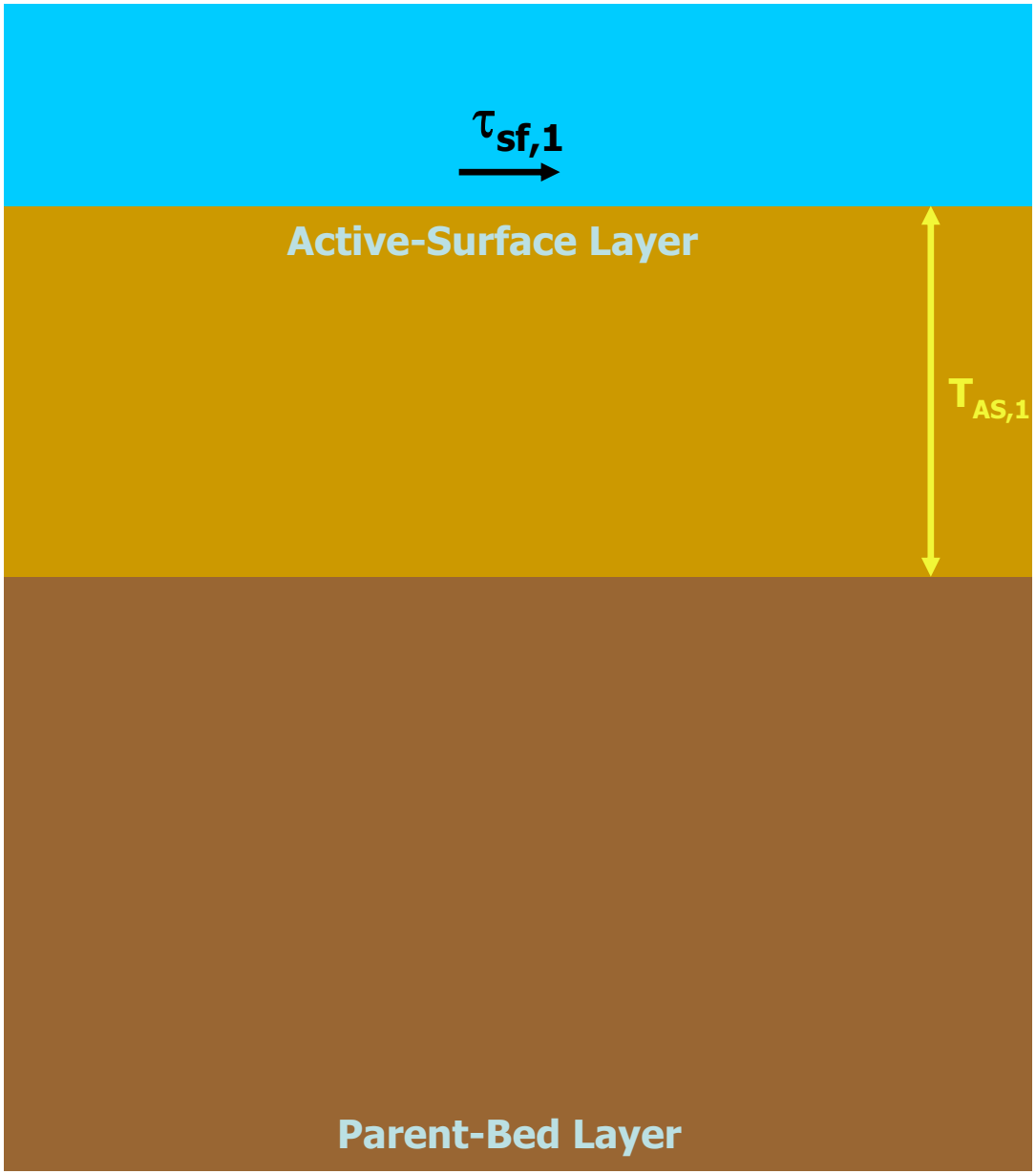

Figure A-8. Initial structure of bed with no active-buffer layer at time = t_1.

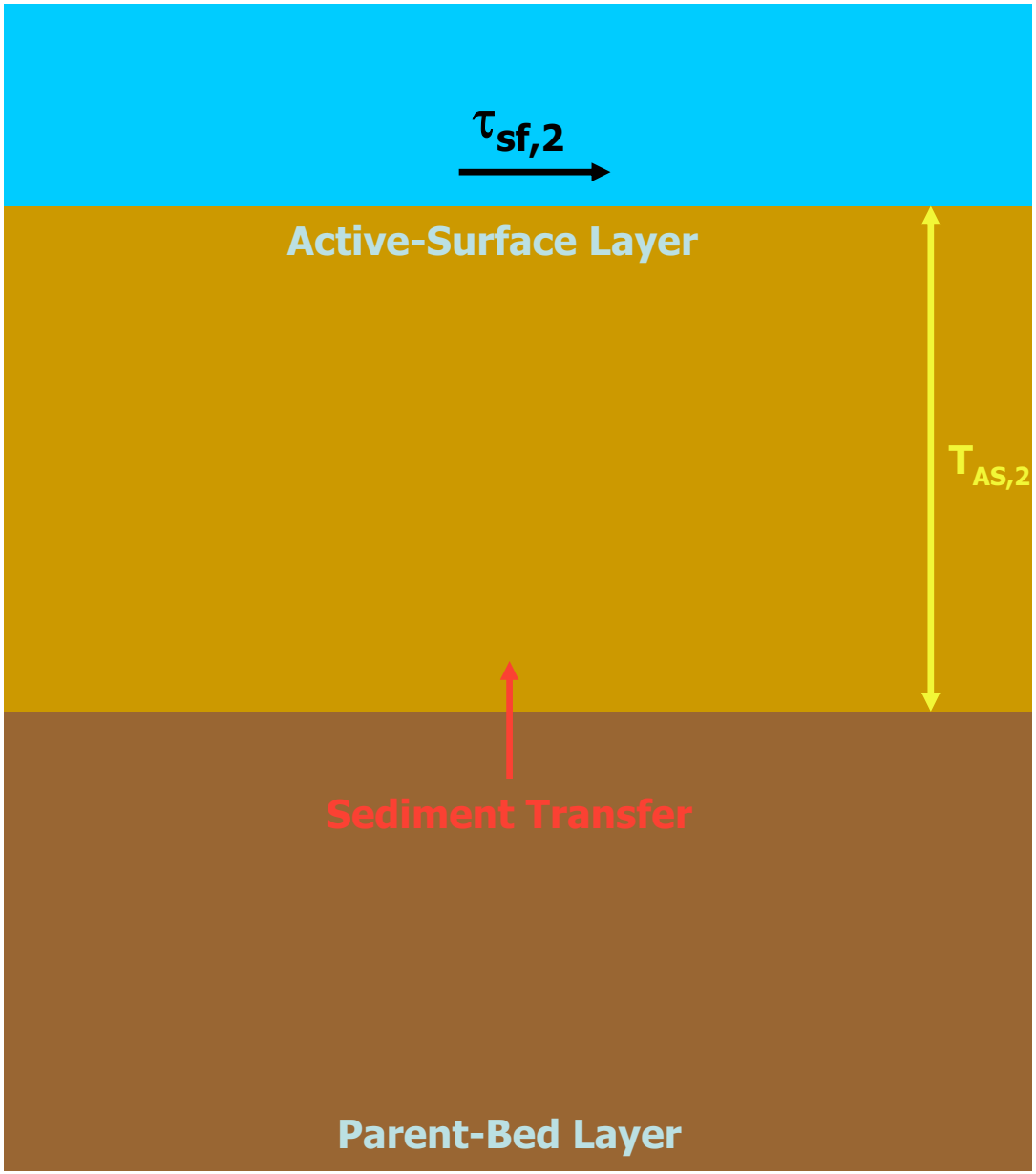

Figure A-9. Active-surface layer thickness increases as shear stress increases ($\tau_2 > \tau_1$) at time = t_2.

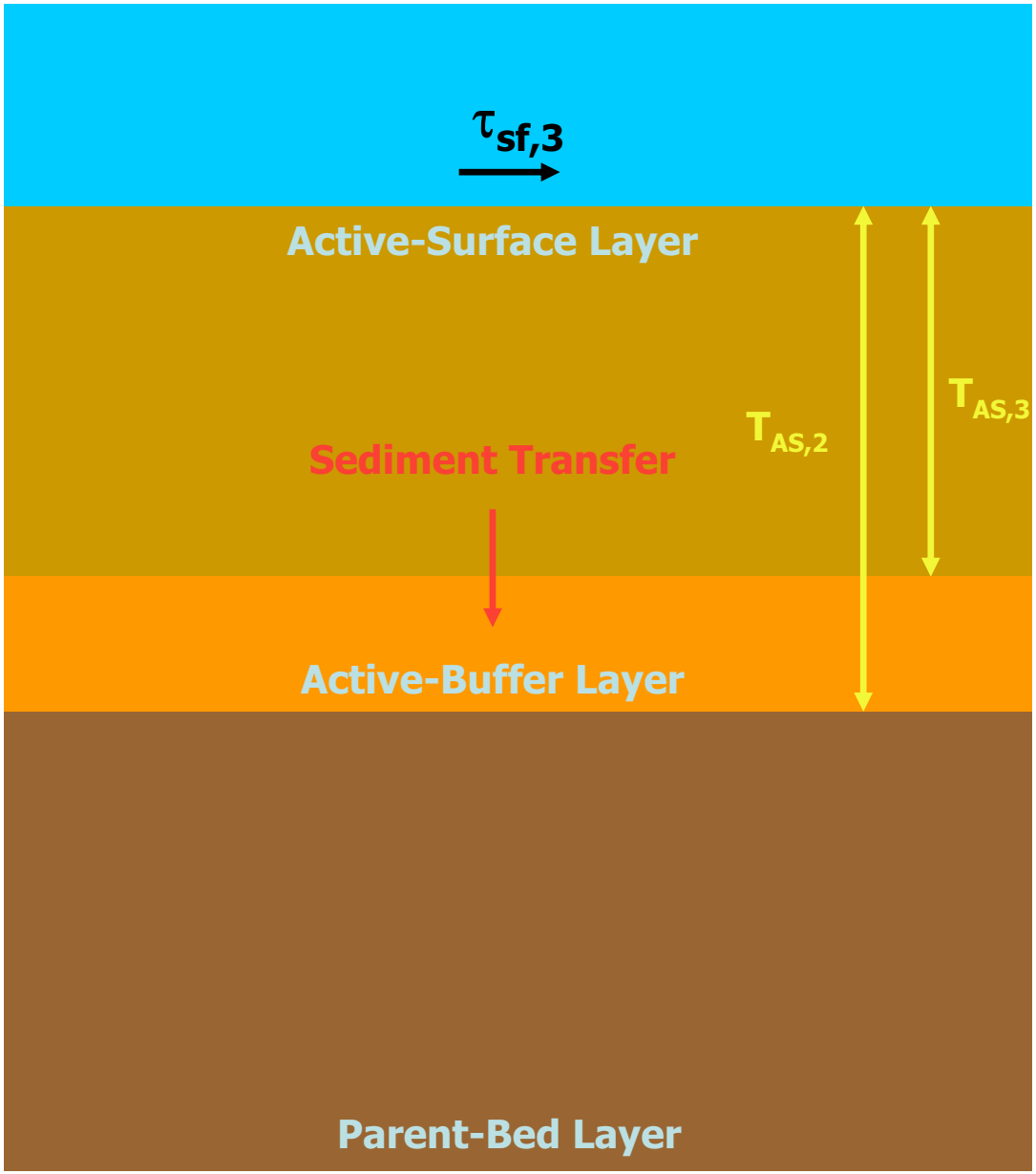

Figure A-10. Active-surface layer thickness decreases and active-buffer layer is created as shear stress decreases ($\tau_3 < \tau_2$) at time = t_3.

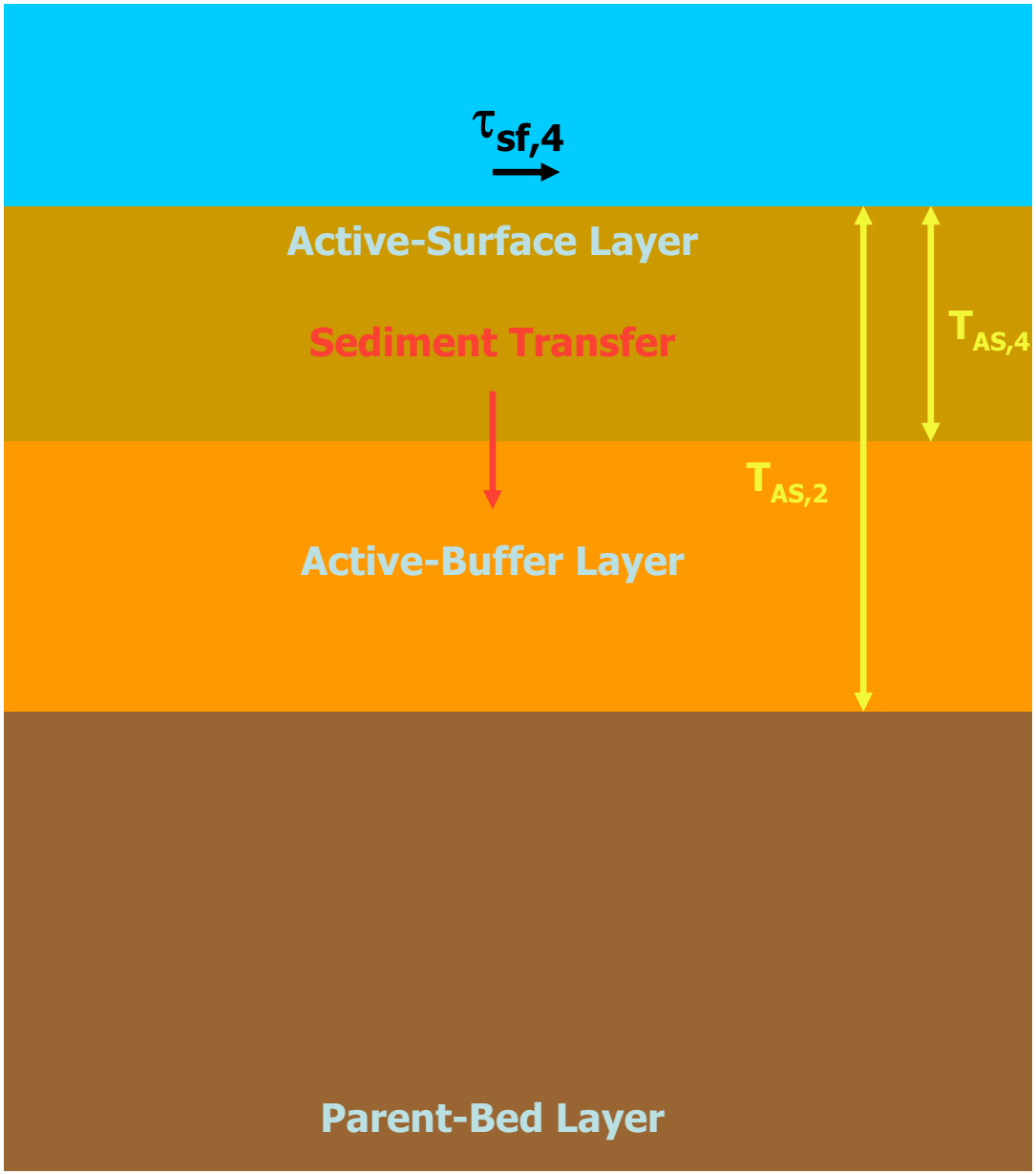

Figure A-11. Active-surface layer thickness decreases and active-buffer layer thickness increases as shear stress continues to decrease ($\tau_4 < \tau_3$) at time = t_4.

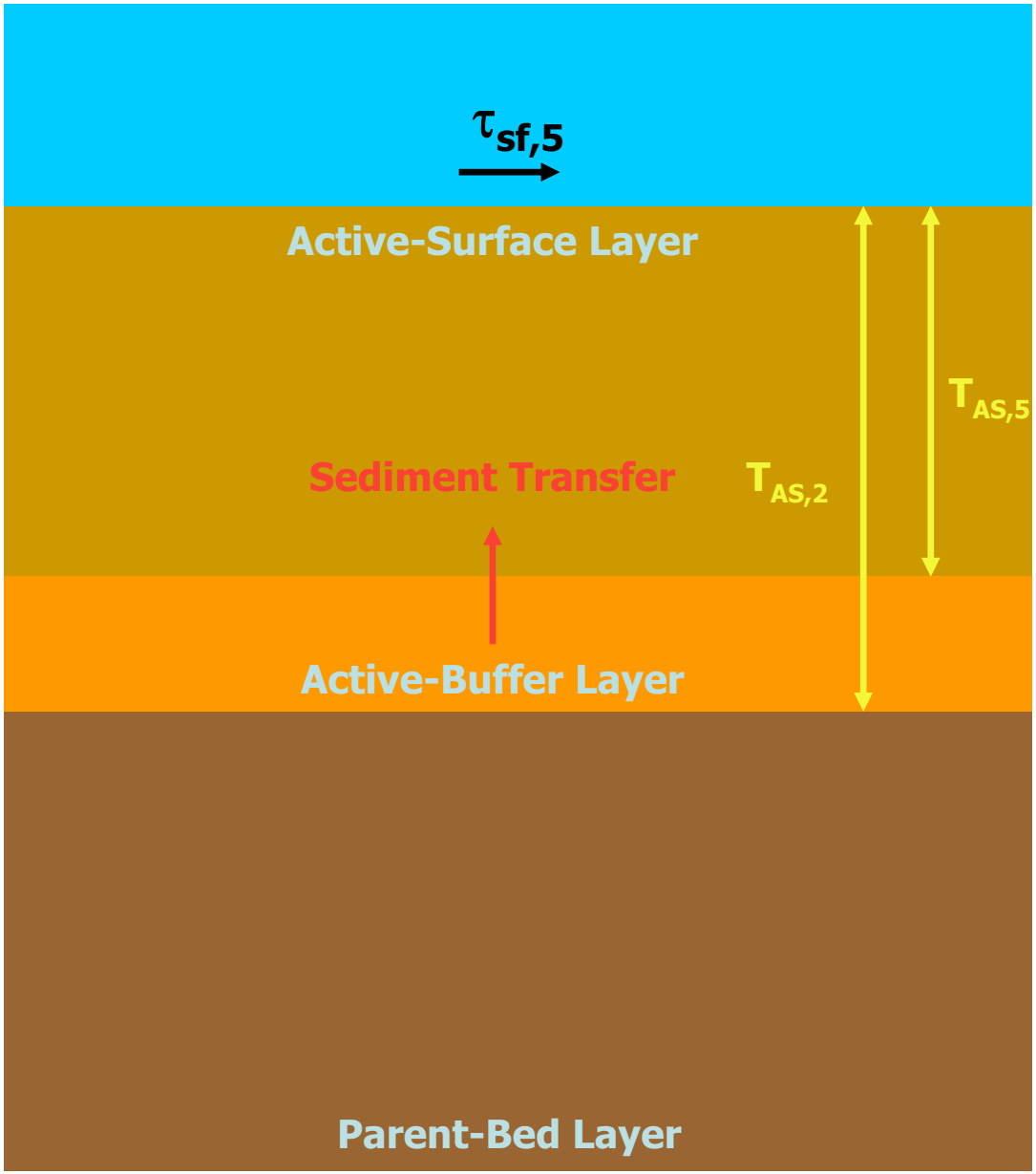

Figure A-12. Active-surface layer thickness increases and active-buffer layer thickness decreases as shear stress increases ($\tau_5 > \tau_4$) at time = t_5.

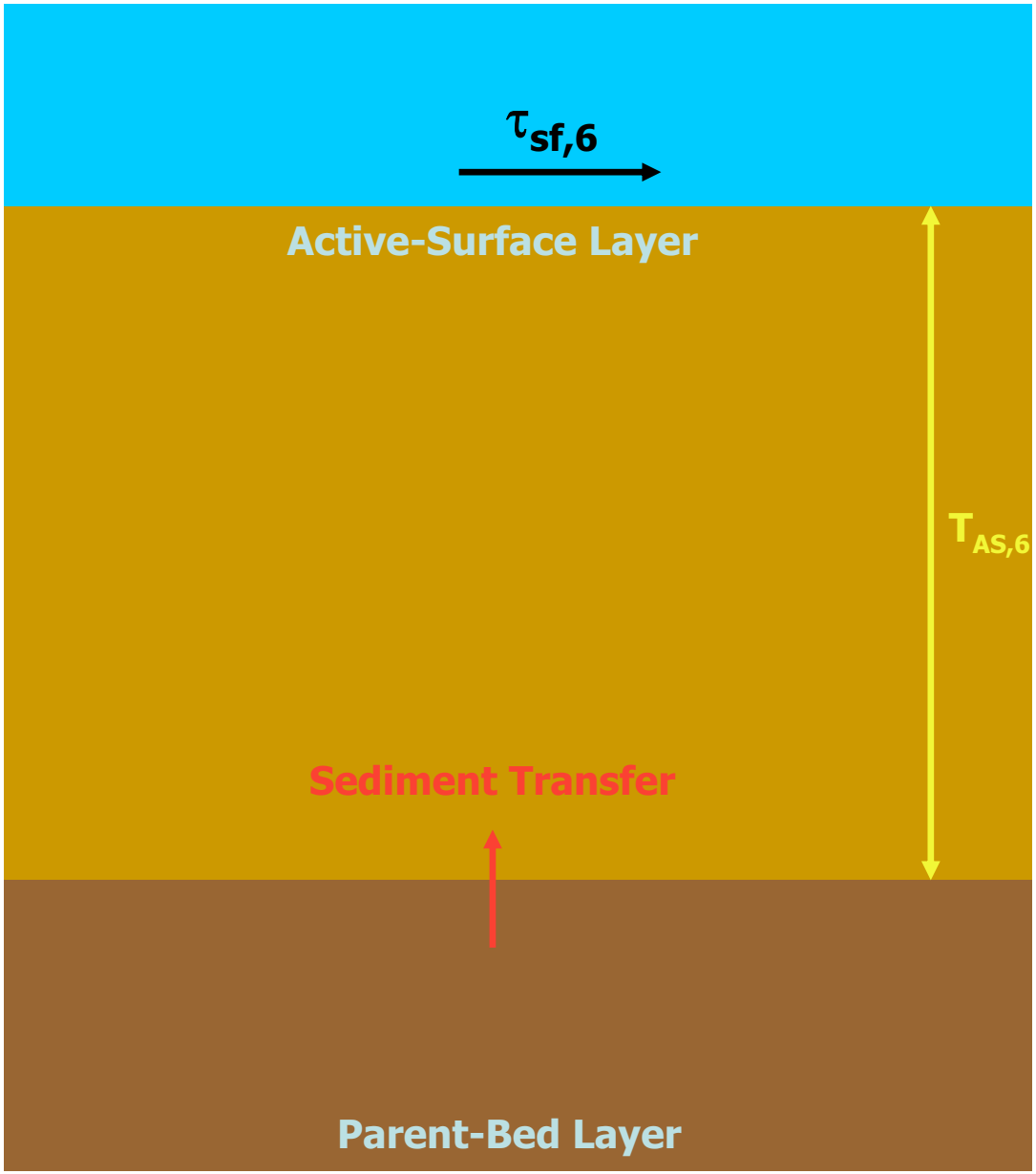

Figure A-13. Active-surface layer thickness increases and active-buffer layer is destroyed as shear stress increases ($\tau_6 > \tau_5$, $\tau_6 > \tau_2$) at time = t_6.

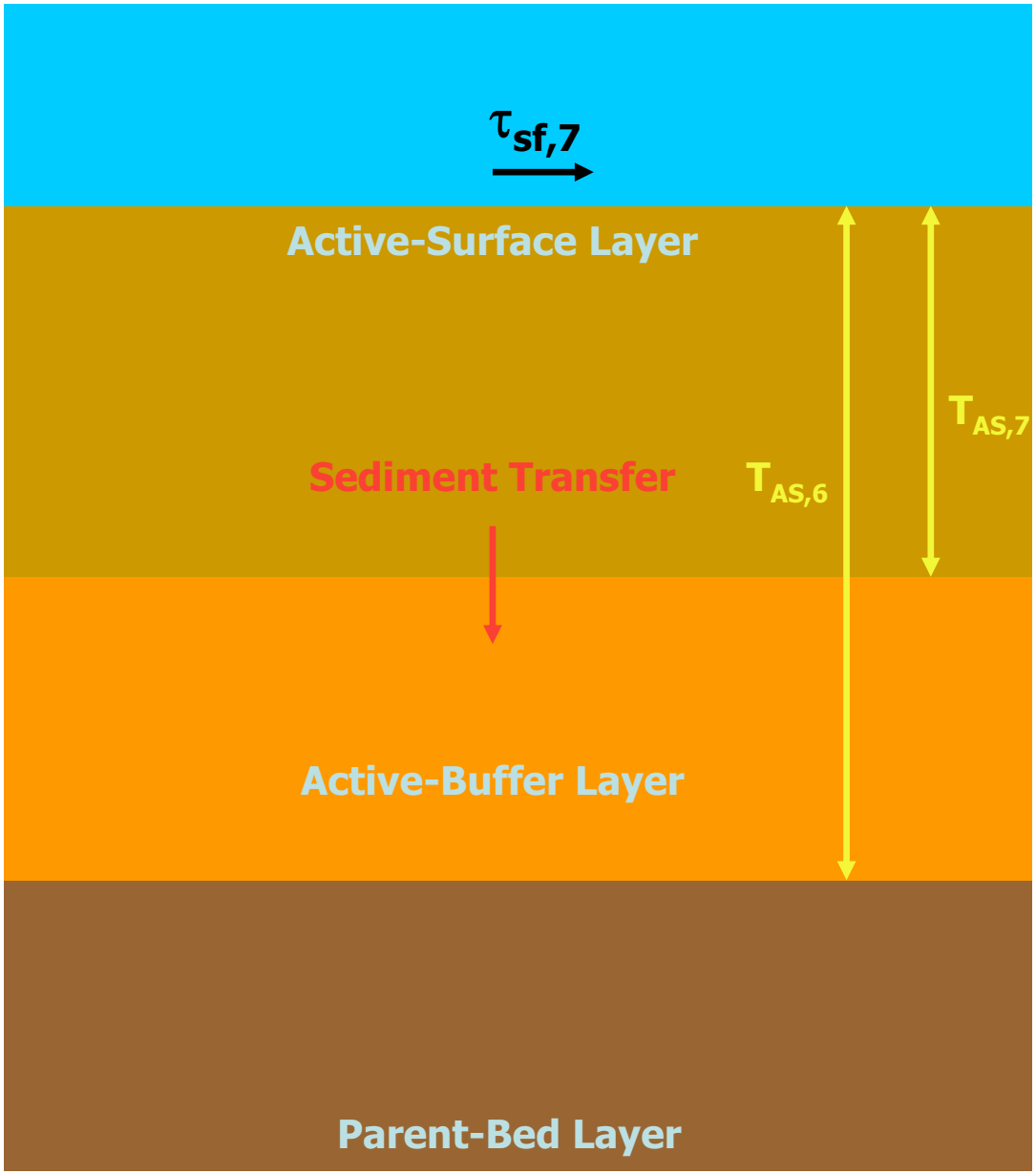

Figure A-14. Active-surface layer thickness decreases and new active-buffer layer is created as shear stress decreases ($\tau_7 < \tau_6$) at time = t_7.

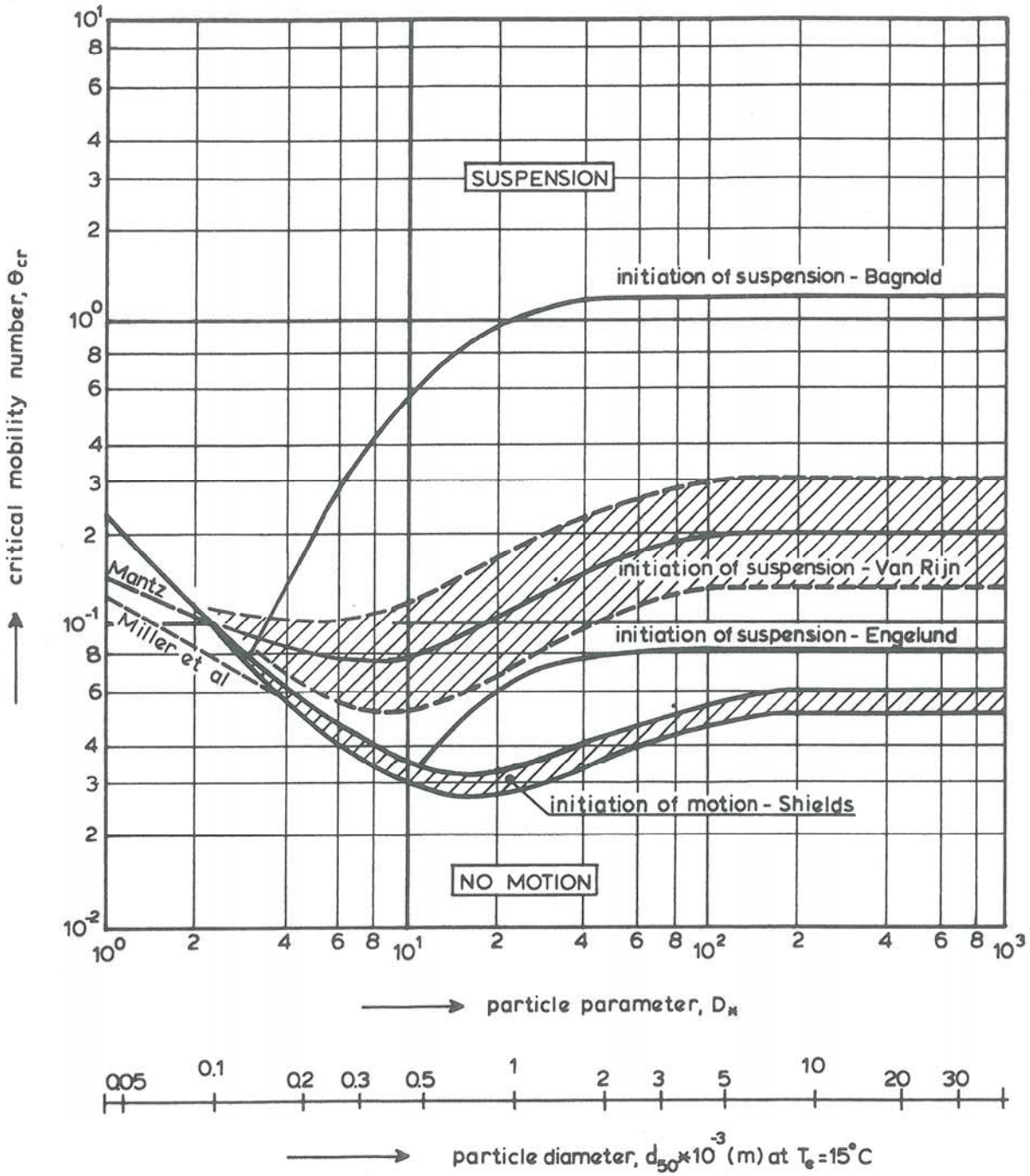

Figure A-15. Initiation of motion and suspension for a current over a plane bed, $\Theta = f(D_*)$, from Van Rijn (1989).

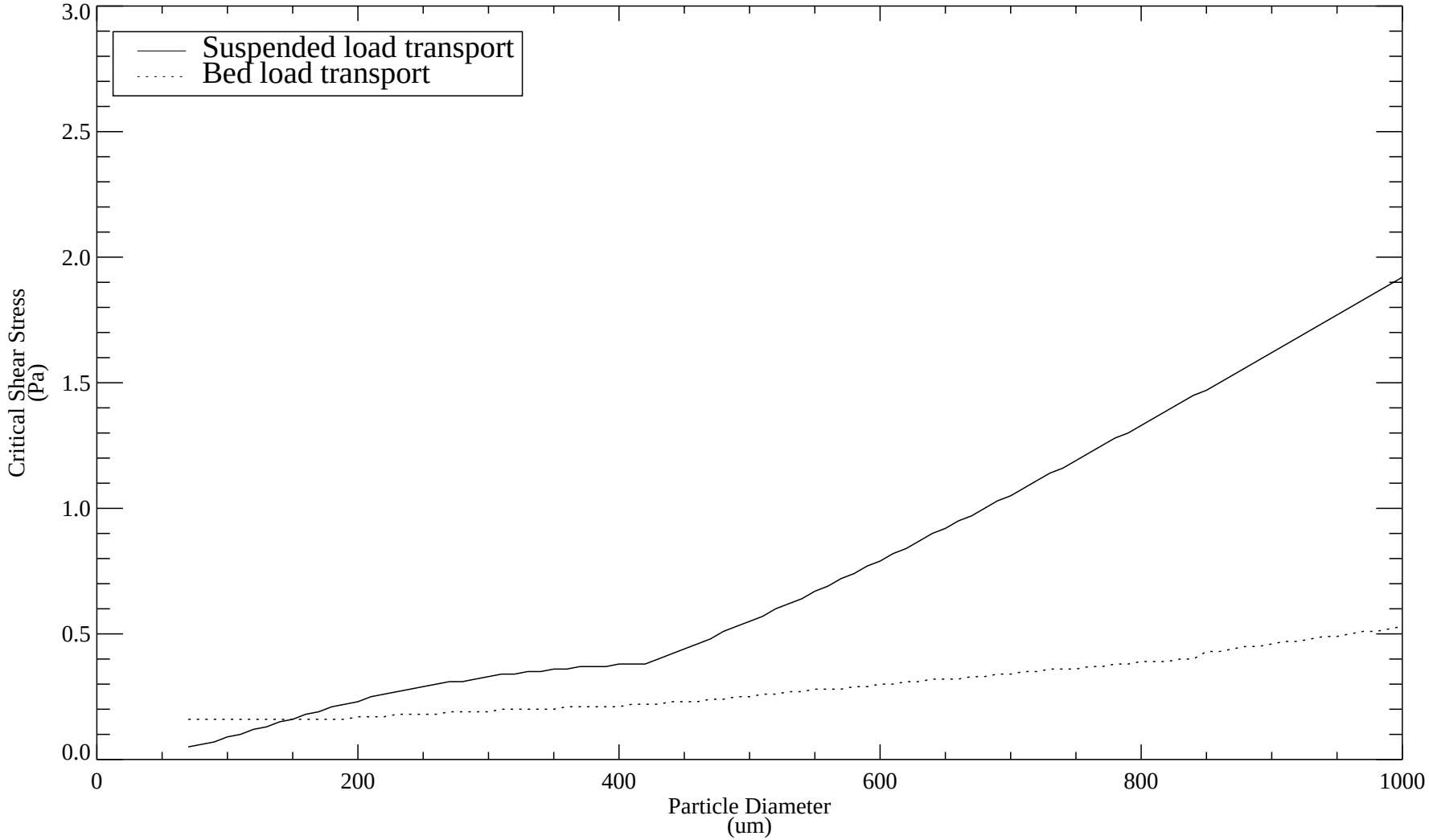

Figure A-16: Critical shear stress for initiation of suspended and bed load transport as a function of particle diameter.

ac - \\Amy\d_drive\RETldw\Anaylsis\Model_Output\plot_tau_susp_vs_bedld_transport_03262007.pro
Thu May 01 14:30:21 2008